SUPPLEMENTARY INFORMATION

Cytosolic nuclease TREX1 C-terminus suppresses immune activation through regulation of oligosaccharyltransferase activity

Maroof Hasan[1,2,@*], Charles S. Fermaintt[1,2*], Ningguo Gao[3#], Tomomi Sakai[4], Takuya Miyazaki[4&], Sixin Jiang[3%], Quan-Zhen Li[5], John P. Atkinson[6], Herbert C. Morse III[4,§], Mark A. Lehrman[3,§] & Nan Yan[1,2,§]

Figure S1-6

Table S1

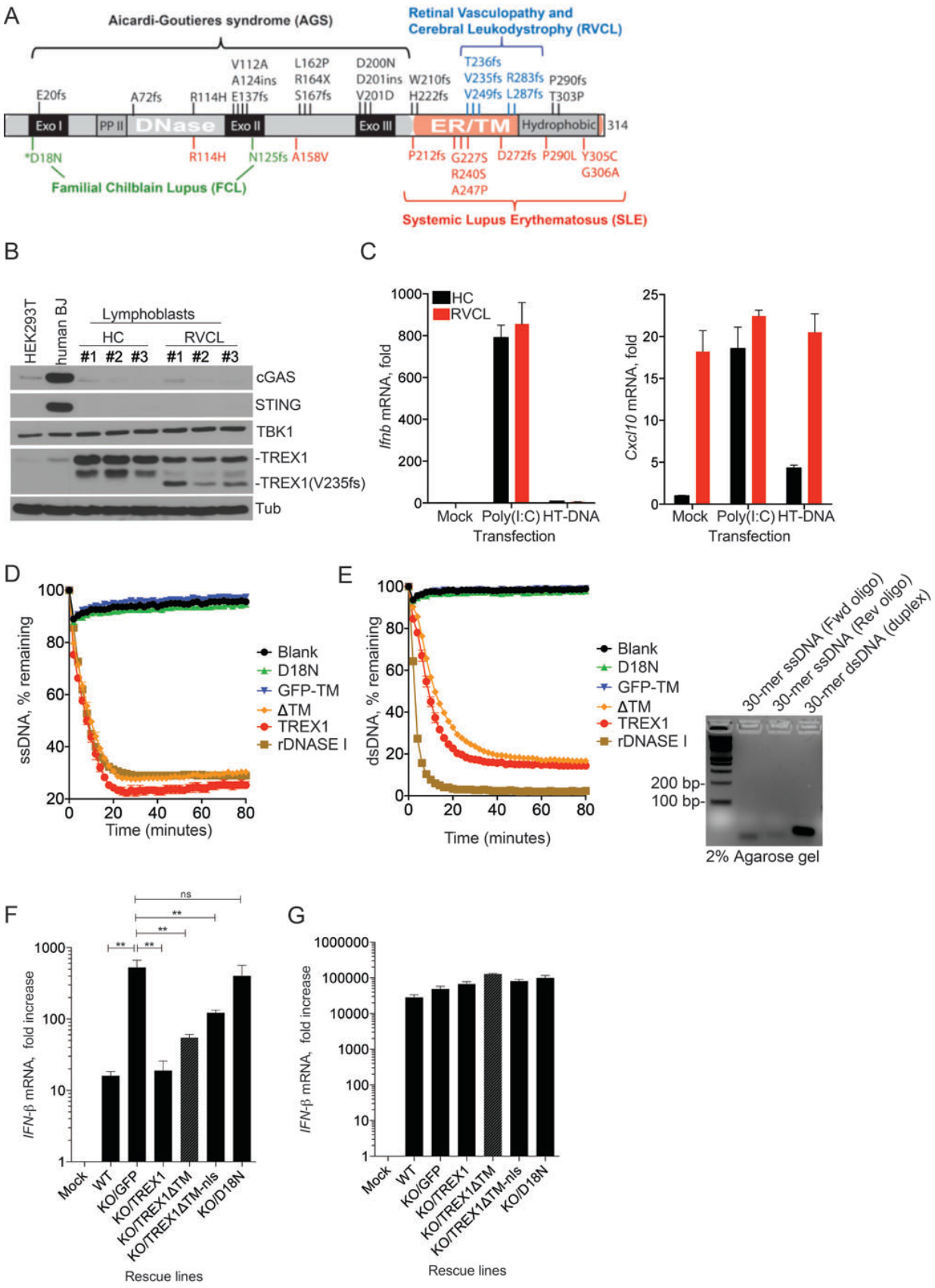
A
Aicardi-Goutieres syndrome (AGS)
Retinal Vasculopathy and Cerebral Leukodystrophy (RVCL)
E20fs
A72fs
R114H
V112A
A124ins
E137fs
L162P
R164X
S167fs
D200N
D201ins
V201D
W210fs
H222fs
T236fs
V235fs
R283fs
L287fs
P290fs
T303P
Exo I
PP II
DNase
Exo II
Exo III
ER/TM
Hydrophobic
314
*D18N
R114H
N125fs
A158V
P212fs
G227S
R240S
A247P
D272fs
P290L
Y305C
G306A
Familial Chilblain Lupus (FCL)
Systemic Lupus Erythematosus (SLE)
B
HEK293T
human BJ
Lymphoblasts
HC
RVCL
#1 #2 #3 #1 #2 #3
cGAS
STING
TBK1
-TREX1
-TREX1(V235fs)
Tub
C
HC
RVCL
Ifnb mRNA, fold
Mock
Poly(I:C)
HT-DNA
Transfection
Cxcl10 mRNA, fold
D
ssDNA, % remaining
Time (minutes)
Blank
D18N
GFP-TM
ΔTM
TREX1
rDNASE I
E
dsDNA, % remaining
30-mer ssDNA (Fwd oligo)
30-mer ssDNA (Rev oligo)
30-mer dsDNA (duplex)
200 bp-
100 bp-
2% Agarose gel
F
IFN-β mRNA, fold increase
ns
**
Mock
WT
KO/GFP
KO/TREX1
KO/TREX1ΔTM
KO/TREX1ΔTM-nls
KO/D18N
Rescue lines
G

Figure S1, related to Figure 1. TREX1 has an DNase-independent function associated with the C-terminus. (**A**) *TREX1* mutations and associated diseases. Note the discordance between AGS mutations falling within the N-terminal DNase domain (Exo I-III), versus RVCL frame-shift mutations at the C-terminal ER/TM localization domain. (**B, C**) Human lymphoblasts do not express key components (cGAS and STING) needed for cytosolic DNA sensing. (**B**) Immunoblots analysis of key proteins required for cytosolic DNA sensing. Positive control is human BJ cells that are fully capable of DNA sensing (Konno et al., 2013). Negative control is HEK293T cells that do not have DNA sensing pathway (Sun et al., 2012). (**C**) Quantitative RT-PCR analysis of *Ifnb* and *Cxcl10* expression after transfection of dsRNA (Poly(I:C)) or dsDNA (HT-DNA). (**D, E**) DNase activity assay. HEK293T cells were transfected with indicated plasmids (all V5-tagged). TREX1 was immunoprecipitated and were incubated with ssDNA (**B**, 30-mer) or dsDNA (**C**, 30-mer duplex with 3' overhang) and monitored in real-time in the presence of SYBR green. See Method for more details. **Right panel**, agarose gel electrophoresis of ss- and dsDNA with Ethidium Bromide staining (that preferentially stains dsDNA duplex). (**F, G**) Quantitative RT-PCR analysis of *Ifnb* mRNA in WT and the indicated *Trex1*$^{-/-}$ rescue MEFs transfected with ssDNA (100-mer, **F**), or with polyI:C (**G**). Logarithmic scales were chosen to present broad ranges of gene expression levels. Results from mock transfected WT cells (Mock) were set to 1. Data are representative of at least three independent experiments. Error bars, SEM.

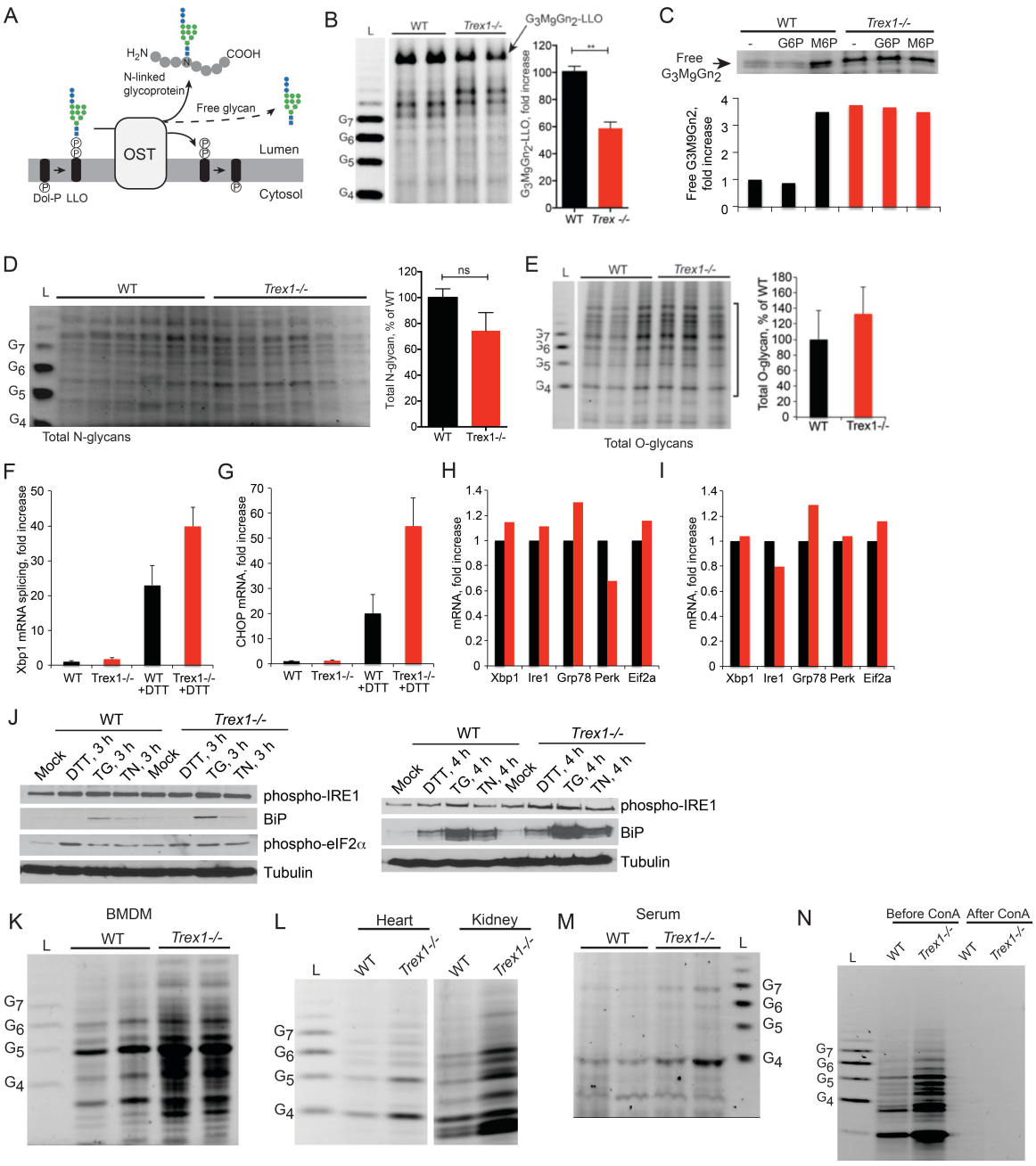

Figure S2, related to Figure 2. OST dysregulation by *Trex1*-deficiency. (**A**) A schematic diagram showing functions of the OST on the ER, including N-linked glycosylation and release of free glycans. (**B**) FACE analysis of LLOs from WT and *Trex1*$^{-/-}$ MEFs. The arrow in **B** indicates $G_3M_9Gn_2$-LLO used for quantification on the right. (**C**) TREX1 suppresses LLO hydrolysis and liberation of free glycans. Plasma membranes of WT or *Trex1*$^{-/-}$ MEFs were selectively permeabilized with streptolysin-O (SLO), and incubated with buffer containing nucleotide-sugars to program LLO synthesis, and used for in-cell LLO hydrolysis assays. Free glycan ($G_3M_9Gn_2$) derived from LLO hydrolysis was protected from

degradation by inclusion of glycosidase inhibitors, and analyzed by FACE. For comparison, mannose-6-phosphate (M6P) was used to stimulate LLO hydrolysis as a positive control (Gao et al., 2011), while glucose-6-phosphate (G6P) served as a nonfunctional control. Quantitation of free glycan was shown below with untreated WT samples set to 1. (**D-E**) Total N-glycans (**D**) and total O-glycan (**E**) from WT and *Trex1*$^{-/-}$ MEFs. No statistical significant differences were observed for total N- or O-glycans between WT and *Trex1*$^{-/-}$ samples. **, $P < 0.01$ (Unpaired t-test, two-tailed). Data are representative of at least three independent experiments (error bars, SEM). **(F-J)**. *Trex1*$^{-/-}$ MEFs do not show signs of ER stress. (**F, G**) Quantitation of *Xbp1* mRNA splicing (**F**) and CHOP mRNA (**G**) expression by qRT-PCR in WT and *Trex1*$^{-/-}$ MEFs that were untreated or treated with 2 mM DTT for 6 hours. Black bars, WT. Red bars, *Trex1*$^{-/-}$. (**H, I**) RNA-SEQ analysis of ER stress related genes in WT and *Trex1*$^{-/-}$ MEFs (**H**) and BMDMs (**I**). (**J**) Immunoblot analysis of ER stress markers in WT and *Trex1*$^{-/-}$ MEFs, with untreated or treated with indicated ER stress inducer for 3 or 4 h. Data in **F** and **G** are representative of two independent experiments. Data in **H** and **I** are data from RNA-SEQ that performed once. **(K-M)** Free glycans are increased in *Trex1*$^{-/-}$ mouse tissues and serum. FACE analysis of free glycan isolated from WT and *Trex1*$^{-/-}$ mouse BMDM (**K**), heart and kidney (**L**) and serum (**M**). Representative images are shown here. Quantitation of three or more independent experiments are shown in **Figure 2B**. We presume that serum free glycans are secreted, and qualitatively distinct from those in mouse cells and tissues due to processing while transiting the secretory pathway. Glucose in serum was removed by a hexokinase/anion exchange step before labeling of the glycans with fluorophore. (**N**) Free glycans bind to ConA. FACE analysis of free glycan isolated from WT and *Trex1*$^{-/-}$ MEFs before or after passing through a ConA column.

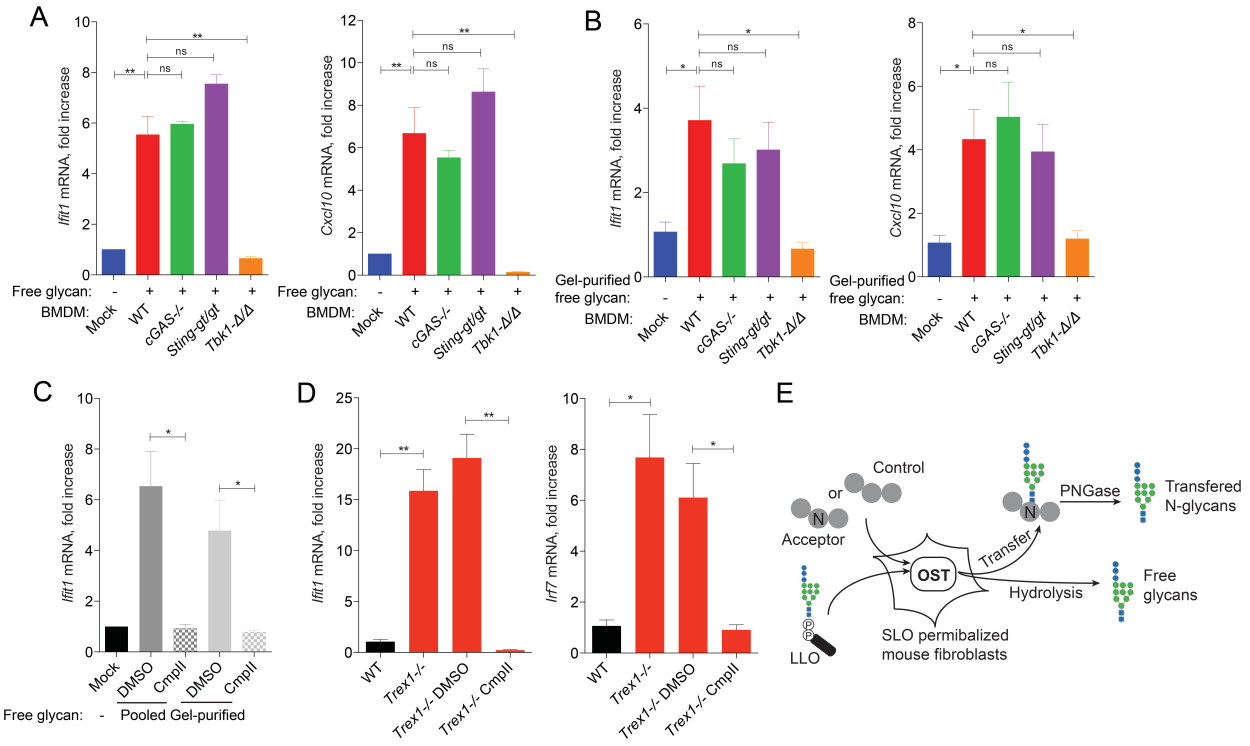

Figure S3, related to Figure 3. Free glycan products from *Trex1*$^{-/-}$ cells stimulate a TBK1-dependent but cGAS/STING-independent innate immune pathway. (**A, B**) Quantitative RT-PCR analysis of immune gene activation in BMDMs treated with free glycans. Free glycan pool (**A**) or gel-purified free glycans (**B**) from *Trex1*$^{-/-}$ MEFs were added to various knockout BMDMs (as indicated). *Ifit1* and *Cxcl10* mRNA expression were measured by qPCR. (**C**) Quantitative RT-PCR analysis of immune gene activation in RAW264.7 cells (a mouse macrophage cell line) treated with free glycans. RAW264.7 cells were treated with a TBK1 inhibitor, Compound II(Ou et al., 2011), at 0.5 uM for 16 h and stimulated with free glycans and measured *Ifit1* mRNA as in **A**. (**D**) TBK1 inhibitor suppresses immune activation in *Trex1*$^{-/-}$ MEFs. WT and *Trex1*$^{-/-}$ MEFs were treated DMSO or Compound II for 16 h and *Ifit1* and *Irf7* mRNA were measured by qPCR. (**E**) A schematic diagram of 'in-cell' OST enzymatic assay used in Figure 3D. Data are representative of at least three independent experiments. Error bars, SEM. Unpaired t-test (**A-D**).

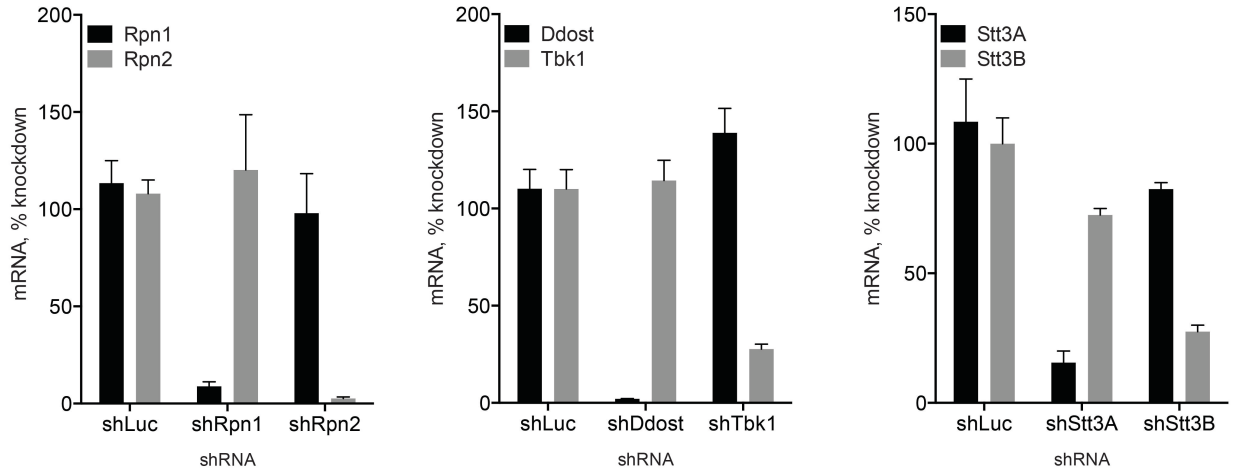

Figure S4, related to Figure 4. shRNA knockdown of OST subunits in *Trex1*$^{-/-}$ cells. *Trex1*$^{-/-}$ MEFs were transduced with lentiviruses expressing specific shRNAs as indicated. Specific knockdown of individual genes was verified by RT-qPCR. Data are representative of two independent experiments.

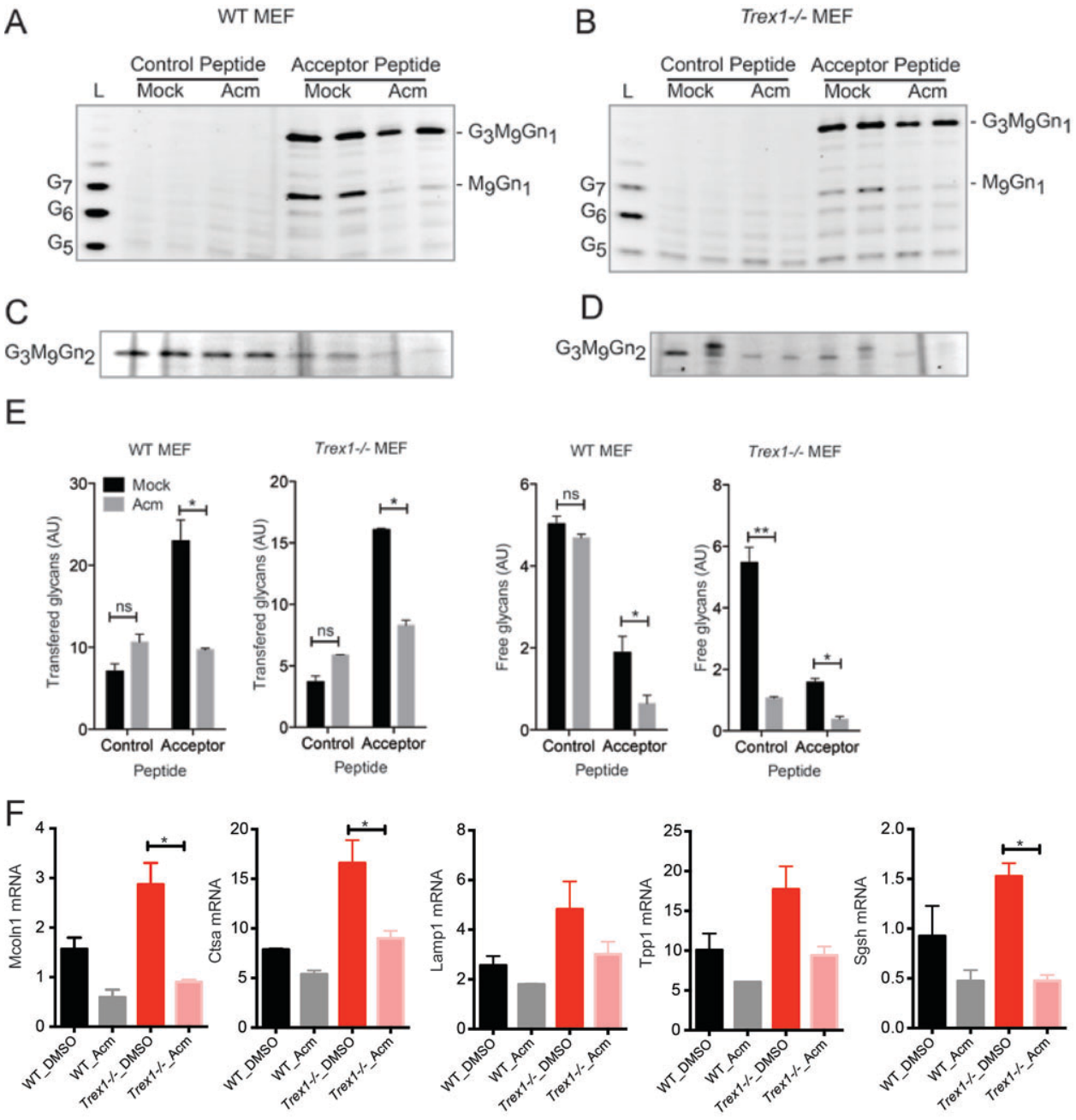

Figure S5, related to Figure 5. Acm inhibits transfer of glycans and LLO hydrolysis by OST, and reduces lysosomal gene expression. (**A,B**) Permeabilized WT or *Trex1*$^{-/-}$ MEFs were incubated with either a control (non-acceptor) peptide, or an acceptor peptide for OST. Glycopeptide products were isolated and then digested with endoglycosidase H (endo H) to release transferred glycans, which were then labeled with ANDS fluorophore for FACE. Since nucleotide sugars were included for continuous synthesis of $G_3M_9Gn_2$-LLO during the reaction, $G_3M_9Gn_1$ is the expected transferred product due to loss of one GlcNAc after endo H digestion. Despite the inclusion of glycosidase inhibitors some glycosidic processing occurs, yielding smaller products including M_9Gn_1 as indicated. Background glycans (control

peptide) reflect glycoproteins present at the beginning of the experiment. **(C,D)** Free $G_3M_9Gn_2$ from the same reactions shown in A and B was analyzed to assess LLO hydrolysis. Panels are aligned with A and B for lane assignments. **(E)** FACE gels in A-D were quantified with ImageJ as arbitrary units (AU), and analyzed statistically by two-way ANOVA. Transferred glycans (E) and Free glycans (F) are plotted. Acm inhibited the ability of OST to both transfer glycan to acceptor peptide, and hydrolyze LLO (transfer of glycan to water). In addition, LLO hydrolysis was reduced by the presence of competing acceptor peptide, a diagnostic indicator of OST function as shown previously (Gao et al., 2005). **(F)** Acm treatment reduces lysosome gene signatures in *Trex1*$^{-/-}$ cells. WT and *Trex1*$^{-/-}$ MEFs were treated with DMSO or Acm for 24 h. Lysosome gene expression was analyzed by qRT-PCR. **P*<0.05, Unpaired t-test. Data are representative of at least two independent experiments. Error bars, SEM.

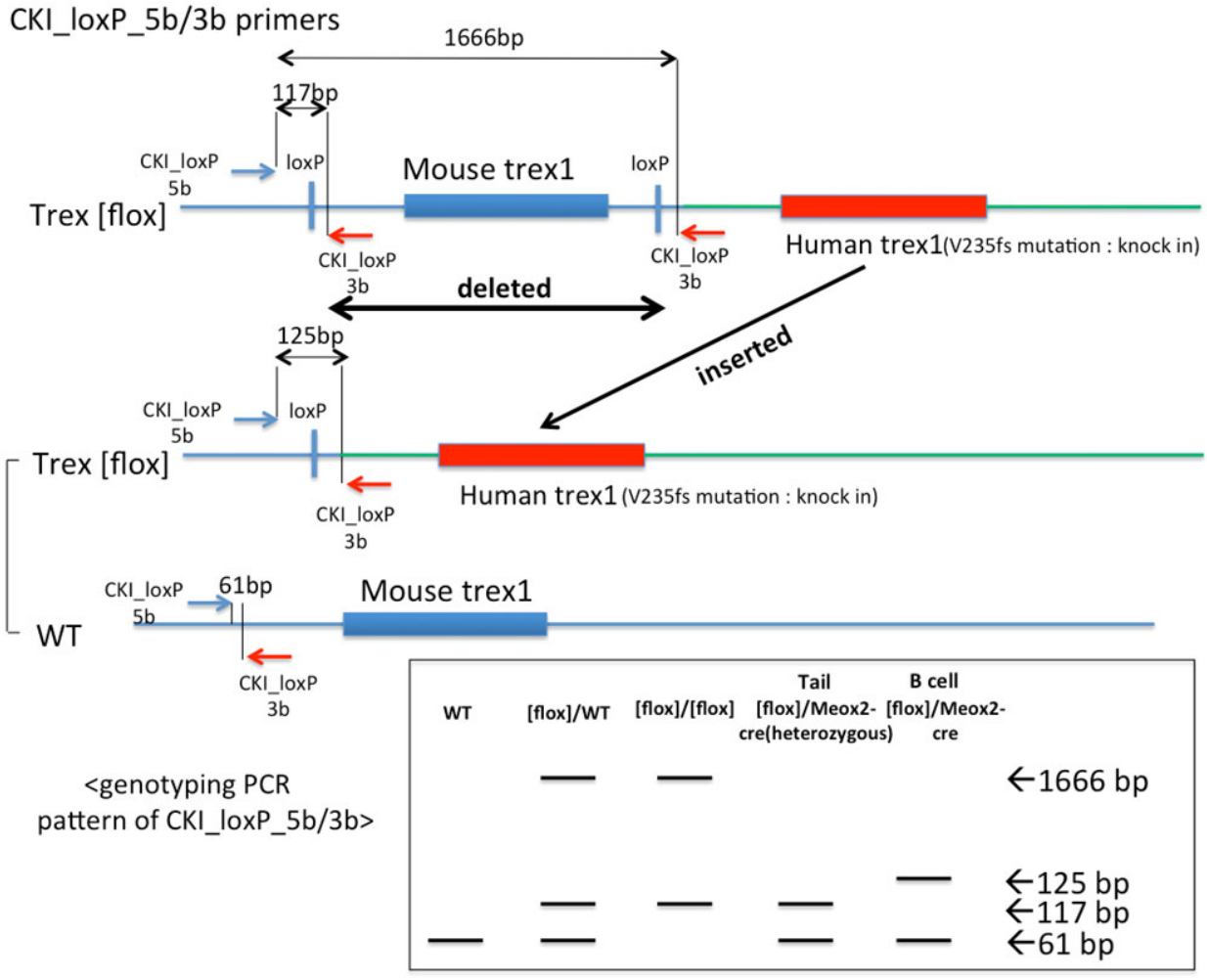

Figure S6, related to Figure 7. *TREX1-V235fs* knock-in design.

Supplementary Table 1, related to Figure 1-7. DNA oligos used in this study. All oligos were purchased from Sigma. qPCR array primer sequences can be requested directly from Bio-Rad.

Oligo name	**Forward and reverse oligo sequence**
Mouse *Gapdh*	TTCACCACCATGGAGAAGGC, GGCATCGACTGTGGTCATGA
Mouse *Ifnb*	CTGCGTTCCTGCTGTGCTTCTCCA, TTCTCCGTCATCTCCATAGGGATC
Mouse *Ifit1*	GAACCCATTGGGGATGCACAACCT, CTTGTCCAGGTAGATCTGGGCTTCT
Mouse *Xbp1*	TGCTGAGTCCGCAGCAGGTG, GCTGGCAGGCTCTGGGGAAG
Mouse Cxcl10	GGGATCCCTCTCGCAAGGACGGTCC, ACGCTTTCATTAAATTCTTGATGGT
Mouse Irf7	TCGCACAGTCTTCCGCGTACCCTGG, TTCCAGCCTCTTCGCTCTCTTCGCT
Mouse Rpn1	GGACCTGAGCAGCCACCTAGCCAAG, ACTTCTAGGTTGTTGTCTTCCTCAT
Mouse Rpn2	ACCCACTACCTCACCAAGCAGGATG, TGGACTGGGCTGCATAGAAGAGAGA
Mouse Ddost	GTGCTGCTGGACAACCTGAACGTGC, TGATGGTCTCCACGTTGATGTTGCC
Mouse Stt3A	TCCACTCGTCTGTTTGCTGT, CAGCCAGGAACCTGGTAGTC
Mouse Stt3B	TCGCTTCTCTCCTTCACCAT, ACCCATGAGATGCAAGATGA
shLuc	CCGGAACTTACGCTGAGTACTTCGACTCGAGTCGAAGTACTCAGCGTAAG TTTTTTTG, AATTCAAAAAAACTTACGCTGAGTACTTCGACTCGAGTCGAAGTACTCAG CGTAAGTT
shRpn1	CCGGCGGGATGAGATTGGTAATGTTCTCGAGAACATTACCAATCTCATCC CGTTTTTG, AATTCAAAAACGGGATGAGATTGGTAATGTTCTCGAGAACATTACCAATC

	TCATCCCG
shRpn2	CCGGGCTGGGCCTCATGTATATCTACTCGAGTAGATATACATGAGGCCCAGCTTTTTG, AATTCAAAAAGCTGGGCCTCATGTATATCTACTCGAGTAGATATACATGAGGCCCAGC
shDdost	CCGGGCCTGACGTGTATGGTGTATTCTCGAGAATACACCATACACGTCAGGCTTTTTG, AATTCAAAAAGCCTGACGTGTATGGTGTATTCTCGAGAATACACCATACACGTCAGGC
shStt3A	CCGGCCCAGTTTGTACGGTTCAGTTCTCGAGAACTGAACCGTACAAACTGGGTTTTTG, AATTCAAAAACCCAGTTTGTACGGTTCAGTTCTCGAGAACTGAACCGTACAAACTGGG
shStt3B	CCGGGGCTTTACTTTGGTCAATTAACTCGAGTTAATTGACCAAAGTAAAGCCTTTTTG, AATTCAAAAAGGCTTTACTTTGGTCAATTAACTCGAGTTAATTGACCAAAGTAAAGCC
ssDNA (30-mer)	TTTTTGGTTTGGTTTTGGCGGAGTTTTCGG
ssDNA Forward oligo (for making dsDNA)	CGGTTTGGTTTTGGCGGAGTTTTCGGGTCGG
ssDNA Reverse oligo (for making dsDNA)	CCCGAAAACTCCGCCAAAACCAAACCGACCG

Supplemental references:

Gao, N., Shang, J., Huynh, D., Manthati, V.L., Arias, C., Harding, H.P., Kaufman, R.J., Mohr, I., Ron, D., Falck, J.R., and Lehrman, M.A. (2011). Mannose-6-phosphate regulates destruction of lipid-linked oligosaccharides. Mol Biol Cell *22*, 2994-3009.

Gao, N., Shang, J., and Lehrman, M.A. (2005). Analysis of glycosylation in CDG-Ia fibroblasts by fluorophore-assisted carbohydrate electrophoresis: implications for extracellular glucose and intracellular mannose 6-phosphate. The Journal of biological chemistry *280*, 17901-17909.

Konno, H., Konno, K., and Barber, G.N. (2013). Cyclic Dinucleotides Trigger ULK1 (ATG1) Phosphorylation of STING to Prevent Sustained Innate Immune Signaling. Cell *155*, 688-698.

Ou, Y.-H., Torres, M., Ram, R., Formstecher, E., Roland, C., Cheng, T., Brekken, R., Wurz, R., Tasker, A., Polverino, T., *et al*. (2011). TBK1 Directly Engages Akt/PKB Survival Signaling to Support Oncogenic Transformation. Mol Cell *41*, 458-470.

Sun, L., Wu, J., Du, F., Chen, X., and Chen, Z.J. (2012). Cyclic GMP-AMP Synthase Is a Cytosolic DNA Sensor That Activates the Type I Interferon Pathway. Science (New York, NY).